ZIBELINE INTERNATIONAL™ PUBLISHING

ISSN: 2521-0890 (Print)
ISSN: 2521-0491 (Online)
CODEN: GBEEB6

Geological Behavior (GBR)

DOI: http://doi.org/10.26480/gbr.01.2024.38.47

RESEARCH ARTICLE

AQUIFER VULNERABILITY STUDIES USING ELECTRICAL RESISTIVITY METHOD IN NSUKKA EAST AND WEST LOCAL GOVERNMENT AREA, ENUGU STATE, NIGERIA

Eni, Oluchi C.*, Ossai, Ngozi M., Ibuot, Johnson C

Department of Physics and Astronomy, University of Nigeria, Nsukka.
Corresponding Email Author: enioluchi2018@gmail.com.

ARTICLE DETAILS

Article History:

Received 20 March 2024
Revised 28 April 2024
Accepted 10 May 2024
Available online 17 May 2024

ABSTRACT

This study utilized electrical resistivity survey methods using the Schlumberger configuration to investigate subsurface formations and assess groundwater vulnerability in the study area. The study employed vertical electrical sounding (VES) with Schlumberger electrode configuration in acquiring the data at ten locations across the study area. The result revealed five geoelectric layers with the fourth layer delineated as the aquifer layers. The values of resistivity and thickness were used in estimating the geohydraulic parameters (Dar-Zarrouk parameters, hydraulic conductivity, porosity, hydraulic resistance and formation factor) which help in evaluating the study area. The values of longitudinal conductance ranged from 0.002 to 0.046 mhos, transverse resistance ranged from 41836.86 to 6462359 Ωm^2, porosity ranged from 7.298 to 19.538 %, formation factor ranged from 0.002 to 0.025, hydraulic conductivity ranged from 0.018 to 0.266 m^2/day and hydraulic resistance ranged from 70.601 to 3895 237. The longitudinal conductance revealed the study area as poorly conducted while the aquifer vulnerability index show low to moderate vulnerability.

KEYWORDS

Aquifer vulnerability, Vertical Electrical Soundings (VES), Dar Zarrouk parameters

1. INTRODUCTION

In the 1980s, private mining in small coal mines was common. Due to the economic and technological constraints at the time, room-and-pillar or tunnel mining methods were often used (Taner et al., 2018; Chopra and Marfurt, 2005). Due to the lack of mining data, the mining scope is no longer known. The remaining goafs will pose great safety hazards to subsequent mine production and construction. Therefore, it is necessary to identify the scope of the goafs to ensure the safe mining of subsequent coal mines (Brown, 1996; Barnes, 1997; Tongjun et al., 2019). A lot of research has been done on the detection and identification of conventional goaf areas, but there is relatively little research on the identification of goaf tunnels (Wiederhold et al., 1998; Jianyuan et al., 2001; Diandong et al., 2001). Geophysical technology is an effective means of measuring underground conditions; the electrical method is very suitable for detecting it; it is water-based, but the detection depth is relatively shallow GPR has a shallow detection depth but can achieve high accuracy the three-dimensional seismic method has a deep detection depth and is the most widely used method (Luo et al., 2006; Yinfeng, 2008; Jin, 2004). Zhang Aimin et al. proposed for the first time the use of three-dimensional seismic technology to directly identify tunnels on time profiles based on tunnel reflection wave characteristics (Wu, 20017). Cheng Jianyuan et al. believe that seismic horizontal slicing is an effective means of detecting tunnels (Dahlke, 2006). Due to the small cross-section of tunnels, tunnels can only be identified on the “three high” seismic data.

Xxx The sharp increase in the quest and global demand for water, reportedly according to the Organisation for Economic Co-operation and Development, is projected to grow by 55% by 2050, disproportionately driven by regions that experience high rates of urbanization and economic growth, many of which can be already classified as water-scarce today (Yee and Le, 2023). Unfortunately, many of the water sources are being polluted, overexploited, and dried up by anthropogenic activities, sometimes with irrevocable consequences. These activities necessitated the dependence on groundwater sources for the much-needed freshwater supplies. According to the U.S. Geological Survey, about 30 percent of the freshwater on Earth is stored in the groundwater in the soil or pores and crevices in the rock, also known as aquifer, which is a body of porous and permeable rock or sediment-saturated with groundwater (The Nature Conservancy, 2023). Also, in comparison to surface water such as rivers and lakes, groundwater refers to the water below the water table in the zone of saturation, moving slowly in the same direction the water table slopes, including the moisture in the pores between soil grains (Obiora and Ibuot, 2020).

Thus, a comparative advantage is that groundwater provides a significant source of fresh water, which may be essential for demands associated with domestic and industrial uses (Machiwal et al., 2018). It is the most accessed global source of freshwater, including drinking water, irrigation, and industrial uses. Groundwater may be recharged by many sources, including rainwater, snowmelt, and water that leaks through the bottom of some lakes and rivers, and the depth of the water table varies depending on several factors such as the physical characteristics of the region, the meteorological conditions, and the recharge and exploitation rates. Also, the groundwater reaching an aquifer does not stand still but normally will keep flowing, albeit much slower than before reaching the aquifer, with the speed of the flow depending on the characteristics of the aquifer and in a direction typically from high to lower levels ruled by gravity, unless there is any anthropogenic impact such as pumping wells. Thus, the groundwater moves until it discharges into another aquifer or another

Quick Response Code	Access this article online	
	Website: www.geologicalbehavior.com	DOI: 10.26480/gbr.01.2024.38.47

Cite The Article: Eni, Oluchi C., Ossai, Ngozi M., Ibuot, Johnson C (2024). Aquifer Vulnerability Studies Using Electrical Resistivity Method In Nsukka East And West Local Government Area, Enugu State, Nigeria. *Geological Behaviour 7(1) : 38-47.*

water body, such as a lake, a river, or the ocean, or until a well extracts it (International Groundwater Resources Assessment Centre, 2022).

However, the quality and quantity of groundwater nowadays are at high risk, particularly threatened directly by activities such as overexploitation, agriculture, population growth, urbanization, wastewater leakage, and indirectly, through climate change, seawater intrusion, and global warming (Chaudhari et al., 2022; Haritash et al., 2017; Machiwal et al., 2018; Nagkoulis and Katsifarakis, 2022; Ncibi et al., 2020). In many African countries, especially the West African states, the continuous uncontrolled dumping of wastes around the environment, accompanied by contamination of surface water mostly due to industrial effluents from industries, thereby contaminating the surface water, has led to over dependence on groundwater as a reliable and safe source of drinking water. Also, many aquifers get depleted over the years, and many aquifers millions of years old contain fossil water and do not recharge, and some aquifer remains dry forever once the water is used up. In some cases where the aquifers naturally recharge, many are depleted at an unsustainable rate (Yee and Le, 2023).

Therefore, making smarter use of the potential of still sparsely developed groundwater resources and protecting them from pollution and overexploitation is essential to meet the fundamental needs of an ever-increasing global population and to address the global climate and energy crises. So, there is a need to protect these aquifers. Thus, the high demand since it is the most reliable and sustainable water source, the lack of abundance of surface water resources, and the lack of knowledge of the nature and identification of subsurface conditions have resulted in the rise in aquifer vulnerability (Singh et al., 2018; Ossai, 2020; Ibuot et al., 2019). Understanding aquifer vulnerability is crucial for sustainable water resource management, especially in areas where groundwater is a significant source of drinking water and agricultural irrigation. Within the Nsukka area of Enugu State, Nigeria, this study aims to evaluate the vulnerability of the aquifers in Nsukka East and Nsukka West to assess the susceptibility of aquifers to contamination from anthropogenic activities and natural processes. The map of the subsurface geological structures will provide valuable insights into the distribution and characteristics of aquifers, such as their depth, thickness, and lateral extent, which are essential for understanding their vulnerability to contamination and identifying potential sources of contamination. The findings can be used to inform land-use planning, water resource management policies, and groundwater protection measures in Nsukka East and West Local Government Area. Ultimately, the goal is to contribute to sustainable development by safeguarding the quality and availability of groundwater resources in the studied area.

2. Geologic Setting Of Study Area

The study area falls within the Lower Benue Trough, comprising of Nsukka East and West Local Government Areas, in the southeastern part of Enugu State Nigeria, with a sedimentary basin extending from the Gulf of Guinea south to the Niger-Benue confluence in the north. The latitude ranges from 6°52'N to 7°28'N, while the longitude ranges from 7°17'E to 7°54'E, and the rocks in the area are predominantly sandstones, shales, and claystone, with some limestone formations in some areas (Figure 1). These sedimentary rocks in the area were deposited during the Cretaceous period and are tilted to the northeast while the aquifers are mainly confined within sandstone formations and recharged by rainfall and infiltration.

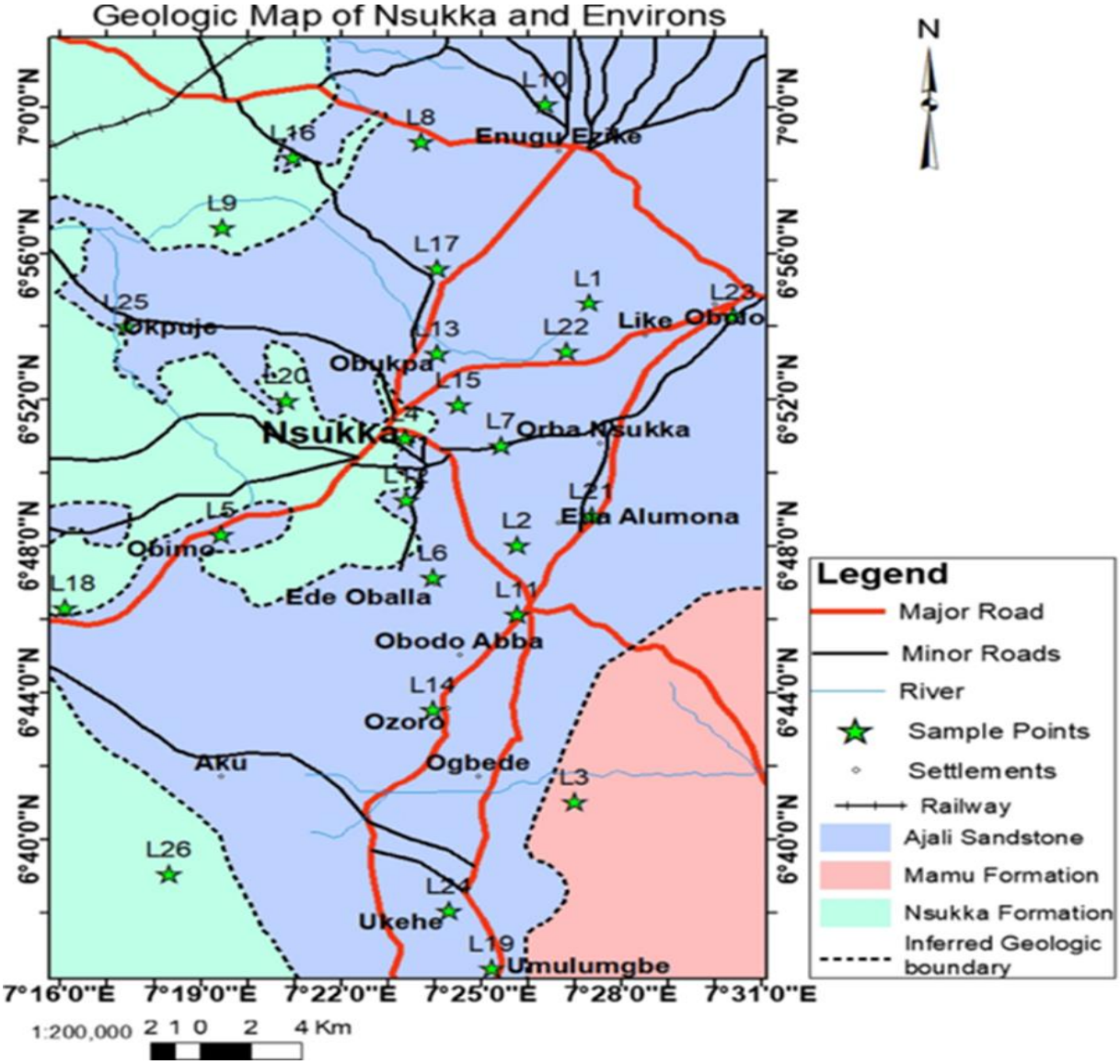

Figure 1: Map showing the location of Nsukka and environs with the major lithostratigraphic units (Onwe et al., 2022).

Geologically, the area lies within the Anambra Basin, an inland sedimentary basin sandwiched between the Southwestern part of the lower Benue Trough and the Petroliferous Niger Delta (Ezim et al., 2017). The area consists of three major geologic formations; Mamu, Ajali, and Nsukka Formations (Ezeh et al., 2010). Two hydro stratigraphic aquifers, namely the upper Maastrichtian Nsukka Formation and middle Maastrichtian Ajali Sandstone both having similar hydraulic characteristics and lithology at depth, where regional saturation occurs (Amah et al., 2016).

3. METHODOLOGY

The electrical resistivity method measures the apparent resistivity of the subsurface, in principle, it measures the voltage generated by a transmission of current between electrodes (Current and potential electrodes) placed in the surface of the earth. In resistivity method, the apparent resistivity (ρ_a) of a medium, which is a function of electrode spacing (Figure 2) is determined using the relationship in equation 1

$$\rho_a = G\frac{\Delta V}{I} \quad (1)$$

Where G is the geometric factor expressed I equation 2.

$$G = \frac{2\pi}{\left\{\left(\frac{1}{AM}-\frac{1}{MB}\right)-\left(\frac{1}{AN}-\frac{1}{NB}\right)\right\}} \quad (2)$$

Apparent resistivity provides a measure of the deviation of the subsurface from the assumed homogenous and isotropic nature. This deviation is called resistivity anomaly and forms the basis of interpretation of resistivity survey.

The Schlumberger configuration which is a widely used method in electrical resistivity surveys was used in this study. It consists of current and potential electrodes, which served as transmitting and receiving electrodes.

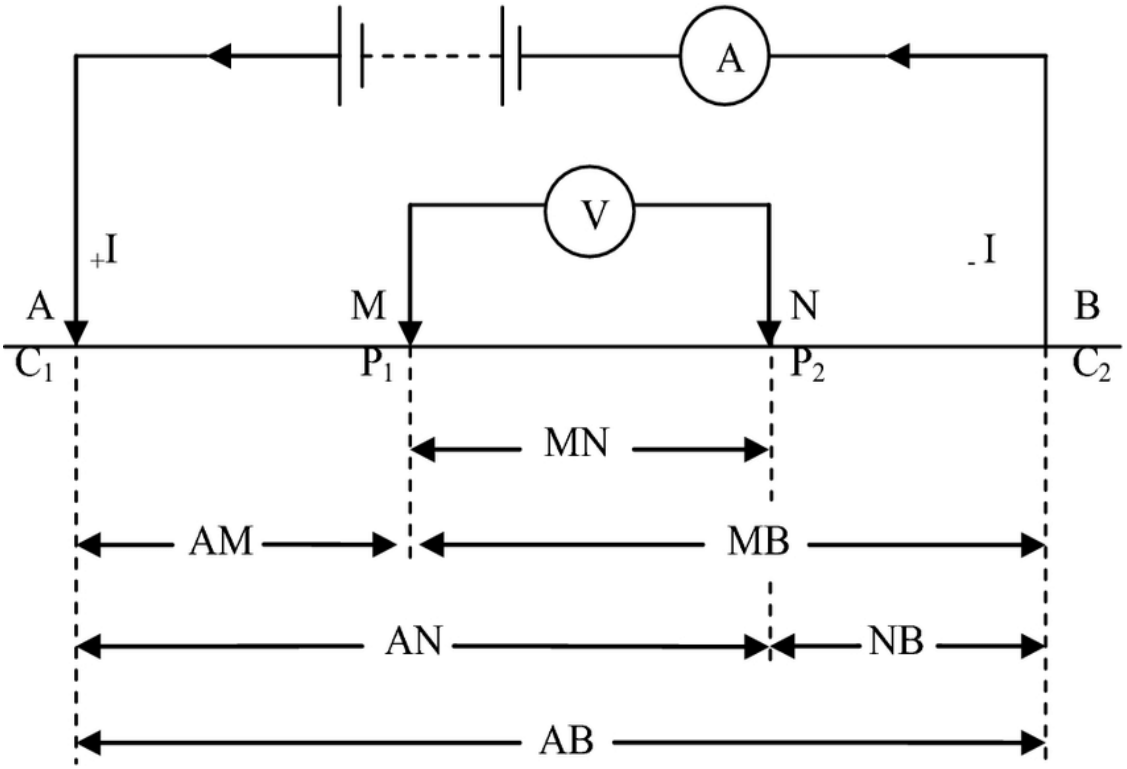

Figure 2: A schematic diagram showing pair of electrodes configuration for resistivity measurements.

During the survey, ABEM SAS 4000 was used to inject current into the ground through the current electrodes (AB), and the potential difference of the subsurface was measured between the potential electrodes (MN). The data were collated by precisely taking the readings of values of the measured resistance R and carefully recording them in the datasheet. The half current electrode spreads (AB/2) ranged from 1.0 to 450.0 m and half potential electrode spreads (MN/2) ranged from 0.25 to 40.0 m. The computation of the apparent resistivity (ρ_a) was done using the values of the apparent resistance (R_a) and geometric factor (G) expressed in equation 3.

$$\rho_a = G.R_a \quad (3)$$

G_S is the geometric factor for the Schlumberger array mainly affected by electrode arrangement, and *Ra* is the field apparent resistance measured from the equipment. Equation (3) can also be written as:

$$\rho_a = \pi\left[\frac{\left(\frac{AB}{2}\right)^2-\left(\frac{MN}{2}\right)^2}{MN}\right]R_a \quad (4)$$

where AB is the distance separating the two current electrodes while MN is the separating distance between the potential electrodes. The field sounding point coordinates were measured using a global positioning system instrument.

3.1 Hydraulic parameters

3.1.1 Porosity

The porosity (Ø) of a geological material is the amount of water (fluid) the material can hold. It can also be referred as the percentage of geological formations hosting an aquifer not occupied by solids. It is expressed as a percentage calculated from the volume of open space in a rock compared with the total volume of the rock. The knowledge of aquifer porosity is fundamental for managing groundwater resources and predicting how contaminants may move through the subsurface. Porosity can be calculated using equation 5 (Maratoz, 1968).

$$\emptyset = 25.5 + 4.5\,In\,K \quad (5)$$

K is the hydraulic conductivity of the aquifer or overlying layer.

The formation factors (F) can be expressed in the simplest form as a power law of the effective porosity and geometric factors using the Archie's law (Archie, 1942). It provides insights into the subsurface properties that influence the movement and storage of groundwater. Equation 6 describes the relationship between formation factor and porosity.

$$F = \frac{a}{\emptyset^m} \quad (6)$$

where a is the pore concentration factor, m is the geometry factor of the pore (empirical constants), and Ø is effective porosity.

3.1.2 Hydraulic conductivity

Hydraulic conductivity (K) is a property of a porous media that reflects the ability of fluids (groundwater) to pass through pores and fractured rocks. It describes with ease fluid can move through pore spaces or fractures. It is a fundamental parameter in hydrogeology, and plays a vital role in understanding and predicting the movement of water through the subsurface. Hydraulic conductivity can be estimated using equation 7 (Heigold et al., 1979).

$$K = 3.86.40\rho_a^{-0.93282} \quad (7)$$

Where ρ_a is the resistivity of the aquifer layer.

3.1.3 Aquifer Vulnerability Index

This parameter assesses the susceptibility of an aquifer to contamination. It provides a quantitative measure of how vulnerable an aquifer is to the potential entry of contaminants from the land surface or other sources. According to a group of researchers, aquifer vulnerability index (AVI) uses the vertical hydraulic conductivity K and the thickness h of the layers overlying the water table to calculate the hydraulic resistance (Stempvoort et al., 1993). The aquifer vulnerability index method measures groundwater vulnerability based on thickness (d) and hydraulic conductivity (K) of the protective aquifer layer/aquitard. Based on the two parameters (d and K), the value of hydraulic resistance, C, can be calculated using equation 8;

$$C = \sum_{i=1}^{n} \frac{d_i}{K_i} \quad (8)$$

Where d_i is the thickness of the protective layer, while K_i is an estimated hydraulic conductivity of the protective layer. Parameter "C" is a theoretical factor to explain the resistance of the aquifer protective layer to vertical flow. The calculated C or log (C) value can be used to produce iso-resistance contour maps. Tables 1 and 2 provide a reference for classifying hydraulic resistance (C) and vulnerability (AVI) based on their corresponding ranges and logarithmic values, respectively.

Table 1: Hydraulic Resistance (C) and Corresponding Log C Values (Stempvoort et al., 1993).

Hydraulic Resistance (C)	Log C
0 – 10	< 1
10 – 100	1 - 2
100 – 1000	2 - 3
1000 - 10,000	3 - 4

Table 2: Vulnerability (AVI) and Corresponding Range

Vulnerability (AVI)	Range
Extremely high	0 – 10
High	10 – 100
Moderate	100 – 1000
Low	1000 - 10,000
Extremely low	> 10,000

3.2 Dar-Zarrok parameters

Dar-Zarrouk parameters are used to characterized the subsurface electrical properties, and defined by longitudinal conductance (S) and transverse resistance (T). Geoelectric unit is characterized by two basic parameters, layer resistivity, and layer thickness which are used to calculate the longitudinal conductance and transverse resistance. These parameters help to evaluate the aquifer layers' protective capacity and its potential (Maillet, 1947; Niwas and Singhal, 1981; Mbonu et al., 1991).

Transverse resistance (T) is used to predict the presence of groundwater, giving its direct proportionality to the aquifer resistivity and thickness, and variations in transverse resistance may indicate changes in lithology, moisture content, or the presence of contaminants. It implies that areas with high transverse resistance will likely have a good quantity of groundwater.

It is evaluated using the equation 9

$$T = \frac{h}{p} \quad (9)$$

where h is the layer thickness in meters, and p is the electrical resistivity of the layer in Ohm-meters.

Also, the longitudinal conductance is used in describing the electrical properties of the subsurface materials. Its values are used in describing the protective capacity of the aquifer layers and it is evaluated using equation 10;

$$S = \frac{h}{\rho} \quad (10)$$

where ρ and h are the layers' resistivity and thickness, respectively.

4. Results And Discussion

The analysis of Vertical Electrical Sounding (VES) data (Table 3) revealed various layers and details on the subsurface resistivity, depth, and thickness of these locations. By analyzing the primary parameters, such as aquifer layer thickness and resistivity values, we determined the overburden layers' resistivity, thickness, and depth values at each location. These bulk parameters were then used to estimate the geohydraulic parameters (Table 4), which helped determine the vulnerability of the aquifer layer to contamination and the protective capacity of the overburdened geoelectric layers. The various geoelectric curves is presented in Figure 3. Five geoelectric layers were delineated with high and low resistivity values at various depths and locations. The resistivity of the layer 1 ranged from 62.0 to 2916.1 Ω m, while the thickness and depth ranged from 0.6 to 2.7 m. The second layer has resistivity, thickness and depth values that ranged from 2818 to 4564.8 Ω m, 2.6 to 17.3 m, and 5.1 to 18.1 m respectively. The third layer resistivity ranged from 612.4 to 42388.6 Ω m while the thickness and depth ranged from l6.3 to 43.1 m and 11.5 to 58.2 m respectively. The fourth Layer with its relatively high thickness compared to other layers was delineated as the aquifer layer with resistivity values ranging from 1787.9 to 51492.9 Ω m, the thickness and depth of this layer ranged from 23.4 to 137.3 and 42.2 to 164.1 m respectively. The fifth layer has resistivity range of 511.7 to 7719.9 Ω m with thickness and depth undefines within the maximum current electrode separation.

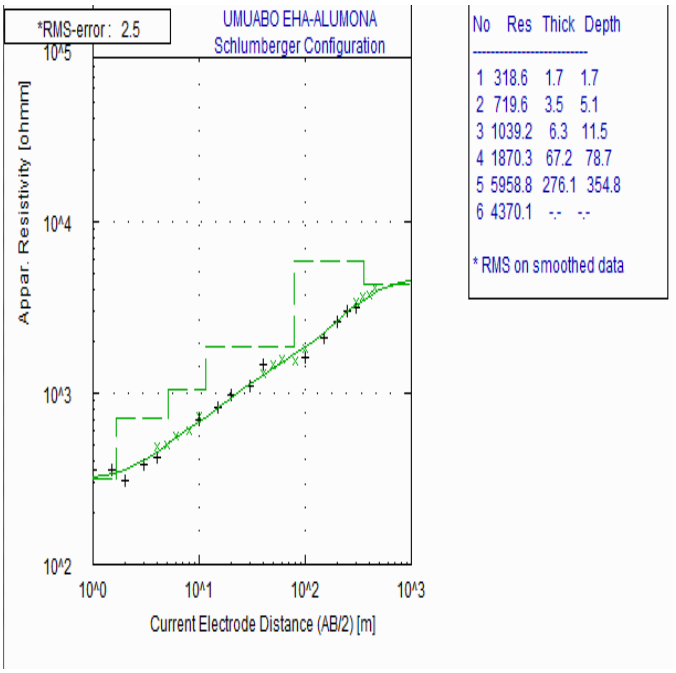

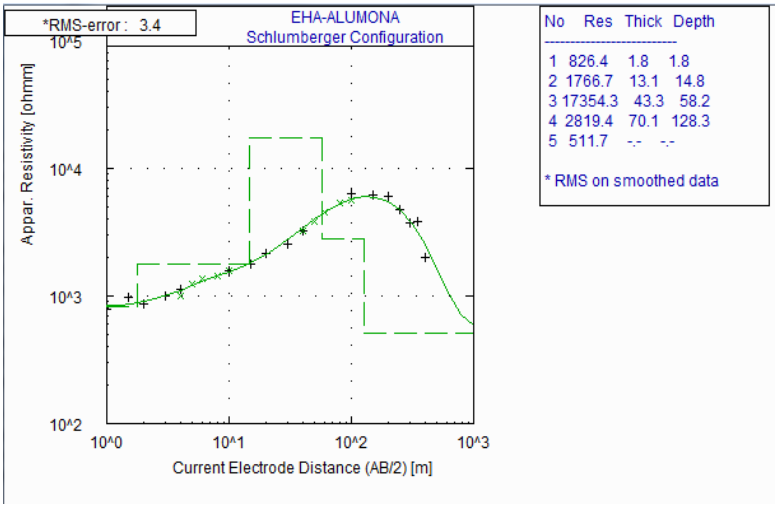

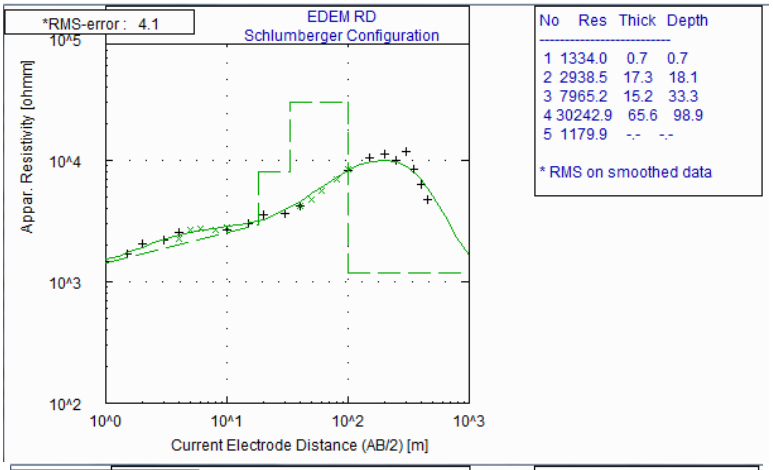

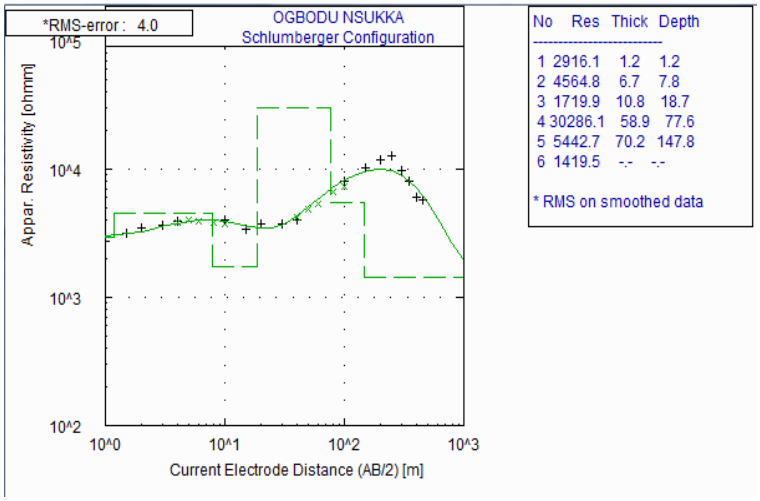

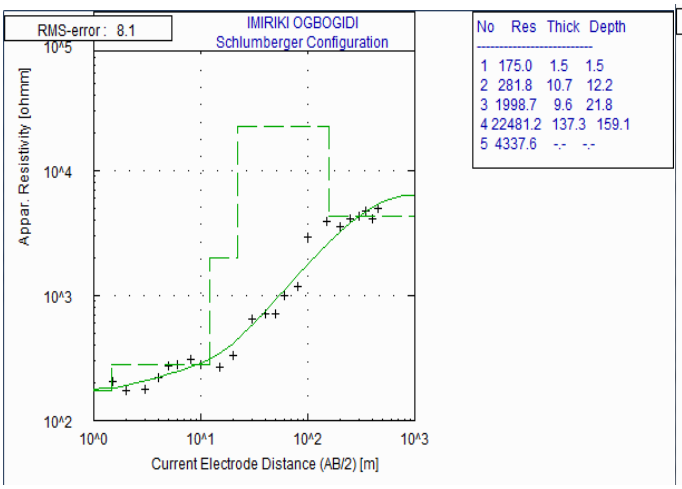

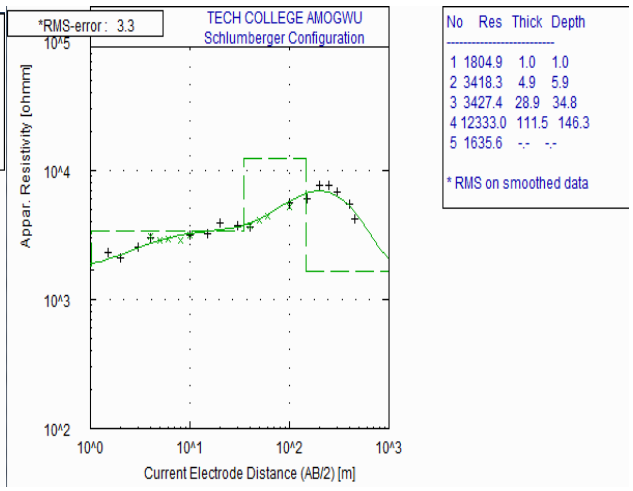

Figure 3: Plots of the geoelectric field some curve models from VES data

Table 3: Summary of geo-electrical characteristics of the Study area obtained from VES Data

S/N	VES points	Longitude (°E)	Latitude (°N)	Resistivity (Ω m)					Thickness (m)				Depth (m)			
				ρ_1	ρ_2	ρ_3	ρ_4	ρ_5	h_1	h_2	h_3	h_4	d_1	d_2	d_3	d_4
1	Agbamere Eha-Alumona	7.4546	6.8275	1197.6	335.2	12417.1	51492.9	7719.9	2.7	5.2	11.6	125.5	2.7	7.8	19.5	144.9
2	UmuaboEha-Alumona I	7.4523	6.8203	318.6	719.6	1039.2	1870.3	5958.8	1.7	3.5	6.3	67.2	1.7	5.1	11.5	78.7
3	Eha - Ndiagu	7.4543	6.8161	826.4	1766.7	17354.3	2819.4	511.7	1.8	13.1	43.3	70.1	1.8	14.8	58.2	128.3
4	UmuaboEha – Alumona II	7.4500	6.8104	719.8	1289.3	1630.9	6163.6	1063.7	1.1	3.6	8.3	102.7	1.1	4.8	13.1	115.7
5	Amagu Ede-Oballa	7.4286	6.8010	62.0	2903.6	612.4	1787.9	7133.6	0.6	3.7	14.4	23.4	0.6	4.4	18.8	42.2
6	Ama - Ezike	7.4194	6.8036	149.5	2803.1	42388.6	2918.4	1738.7	1.7	2.6	43.1	116.7	1.7	4.3	47.4	164.1
7	Edem Ani	7.3759	6.8652	1334.0	2938.5	7965.2	30242.9	1179.9	0.7	17.3	15.2	65.6	0.7	18.1	33.3	98.9
8	Ogbodu Nsukka	7.3689	6.8717	2916.1	4564.8	1719.9	30286.1	5442.7	1.2	6.7	10.8	58.9	1.2	7.8	18.7	77.6
9	Imiriki Ogbogidi	7.3604	6.8781	175.0	281.8	1998.7	22481.2	4337.6	1.5	10.7	9.6	137.3	1.5	12.2	21.8	159.1
10	Tech College Amogwu	7.3543	6.8543	1804.9	3418.3	3427.4	12333.0	1635.6	1.0	4.9	28.9	111.5	1.0	5.9	34.8	146.3

Table 4: Summary of the Calculated DarZarrok aquifer geo-hydraulic parameters from resistivity and thickness of aquifer layer

VES	VES Stations	Long. (°E)	Lat. (°N)	Overburden Resistivity ρ (Ωm)	Overburden Thickness h (m)	Hydraulic conductivity K (m/day)	Porosity	Formation Factor	Long. Cond. S (Ω^{-1})	Trans. Resist. T ($\Omega\ m^{-2}$)	Protective Capacity	Hydraulic Resistance (C)	Log C	AVI Rating
1	Agbamere Eha- Alumona	7.4546	6.8275	13949.9	19.5	0.053	12.246	0.012	0.002	6462359	POOR	370.833	2.569	Moderate
2	Umuabo Eha-Alumona	7.4523	6.8203	3947.7	78.7	0.171	17.545	0.007	0.046	1645225	POOR	461.015	2.664	Moderate
3	Eha- Alumona	7.4543	6.8161	19947.4	58.2	0.038	10.745	0.014	0.025	197639.9	POOR	1545.072	3.189	Low
4	UmuaborEhaalumona II	7.4500	6.8104	3640	13.0	0.184	17.886	0.007	0.017	633001.7	POOR	70.601	1.849	Moderate
5	Ede Oballa	7.4286	6.8010	3578	18.7	0.187	17.958	0.007	0.013	41836.86	POOR	99.942	2.000	Moderate
6	Ama- Ezike	7.4194	6.8036	45341.2	47.4	0.018	7.298	0.025	0.040	340577.3	POOR	2706.809	3.433	Low
7	Edem Rd	7.3759	6.8652	12237.7	33.2	0.059	12.796	0.011	0.002	1983934	POOR	558.766	2.747	Moderate
8	Ogbodu	7.3689	6.8717	39486.9	77.6	0.020	7.878	0.023	0.013	382077.5	POOR	3895.237	3.591	Low
9	Imiriki Ogbogidi	7.3604	6.8781	2455.5	21.8	0.266	19.538	0.006	0.006	3086669	POOR	82.006	1.914	Moderate
10	Tech College Amogwu	7.3543	6.8543	8650.6	34.8	0.082	14.252	0.009	0.009	1375130	POOR	423.777	2.627	Moderate

4.1 Overburden layer result

The values of resistivity and thickness of the layers situated above the aquifer were summed up and the values presented in Table 4. The contour map (Figure 4) highlighted the spatial distribution of the overburden resistivity across the study area, indicating the prevalence of moderate resistivity values. Specifically, VES 6 and its surrounding area exhibited the highest overburden layer resistivity which is observed in the southern part of the study area. This could be attributed to the compact nature of the subsurface and the type of geomaterials present. The overburden layers thickness displayed a range of 13.0 to 78.7 m, with VES 3 and 6 showing the highest values. The spatial distribution of the overburden layers thickness (Figure 5) depicts an area with varying thicknesses of layered material, ranging from high to low. Interestingly, the areas with high overburden resistivity did not necessarily correspond to areas with high overburden thickness, and vice versa. Notably, the aquifer units in areas with high overburden thickness may be regions with prolific aquifer. At the same time, the overburden layers contain more contaminated conducting fluids than the aquifer layer. The thickness of the overburden layer plays a crucial role in aquifer vulnerability assessment as it acts as a barrier, delaying the travel time of contaminants to the aquifer and reducing their potential impact (Levison and Novakowski, 2009; Hussain et al., 2019; Ossai et al., 2020)

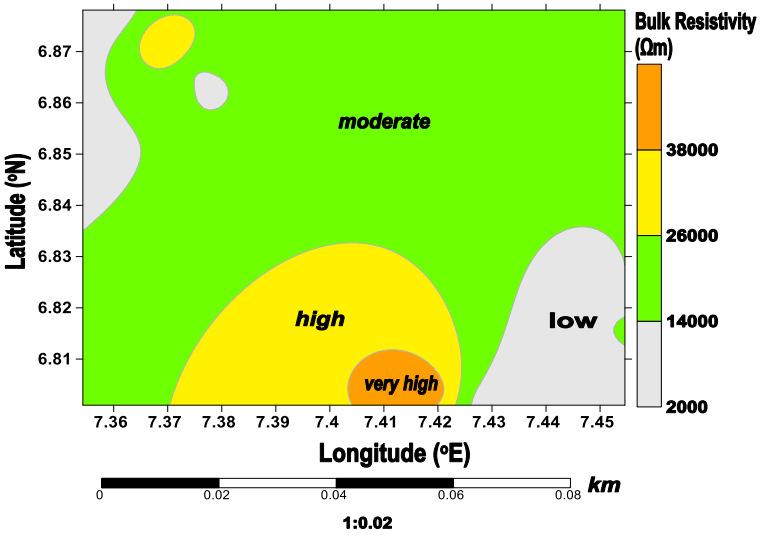

Figure 4: Contour maps of overburden layers resistivity

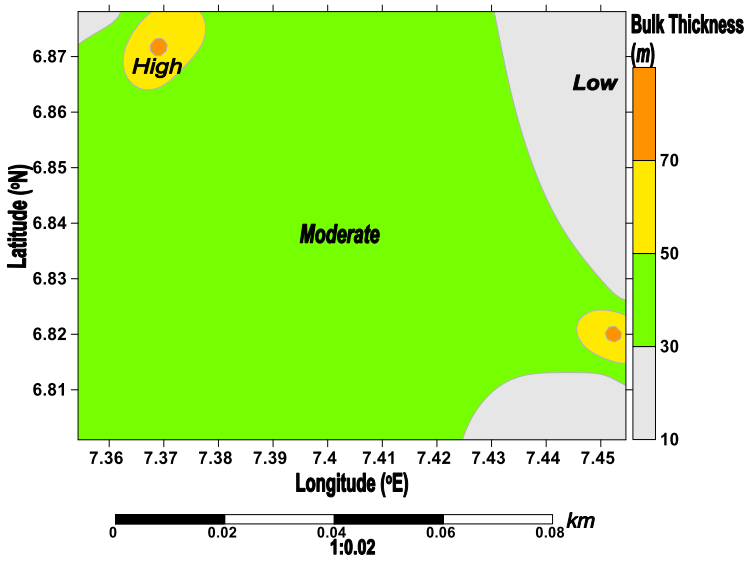

Figure 5: Contour maps of over burden layer thickness

The estimated hydraulic conductivity values (K) for the overlying layer vary across the surveyed locations. The lowest value of 0.018 m/day was observed Ama- Ezike, while the highest value of 0.266 m/day was recorded at Imiriki Ogbogidi. High values of hydraulic conductivity indicate the presence of permeable materials that allow water to flow quickly, while low values suggest less permeable materials. The contour map depicted in Figure 6 shows that the northwest and southeast of the study area exhibits the highest values of overburden hydraulic conductivity. It implies that these locations have favorable conditions for groundwater accumulation, indicating prolific aquifer in these areas. The hydraulic resistance, a key parameter in assessing groundwater vulnerability and indicating the protective capacity of the aquifer layer, was also estimated and the values ranged from 70.601 to 3895.237. This help in determining the aquifer vulnerability index (AVI) which delineated the study area into low and moderate vulnerability class. This classification provides insights into the vulnerability of the aquifers in these areas to potential contamination. This parameter plays a significant role in evaluating geomaterials' ability to impede the infiltration of fluids into the subsurface, as they naturally act as filters for percolating fluids (Mogaji et al., 2007 in Ibuot et al., 2019). Figure 7 is a contour map depicting the distribution of hydraulic resistance across the study area, it reflects the variation in AVI across different zones. It highlights the regions characterized by low to moderate protective capacity, indicating their vulnerability to contamination. These findings align with previous works by groups of researchers which also emphasize the susceptibility of such zones to groundwater pollution (Braga et al., 2006; Ehirim and Nwankwo; 2016; George, 2021). Conversely, areas with high-resistive materials exhibit low hydraulic resistance and conductive fluids, suggesting they may not be ideal for drilling boreholes with high yield expectations (Mbonu et al., 1991 in Obiora et al., 2018).

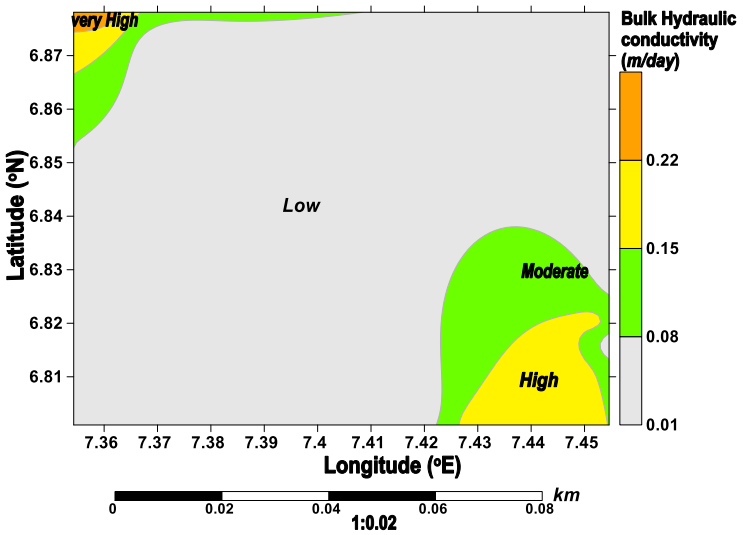

Figure 6: Contour map of bulk hydraulic conductivity

Porosity and formation factor, which describe the characteristics of the overburden layers, were also estimated and their values ranged from 7.298 to 19.538 % and 0.002 to 0.025 respectively. The variation and distribution of these parameters (Figures 8 and 9) provide valuable insights into the spatial distribution of these geo-hydraulic properties across the study area. The overlaying layer's porosity influences the fluid's during infiltration. Low to moderate porosity level sweeps across the area except for some parts in the northwestern and southeastern region with high porosity levels which corresponds to regions of high hydraulic conductivity, affirming that a highly porous layer allows free flow of fluids. On the contrary, areas with high formation factors in Fig. 9 also correspond to areas with high thickness and resistivity. In contrast, high porosity areas are attributed to areas with low formation factors and vice versa. When the formation factor of an area is very high, the hydraulic conductivity, transmissivity, permeability, and porosity will be very low.

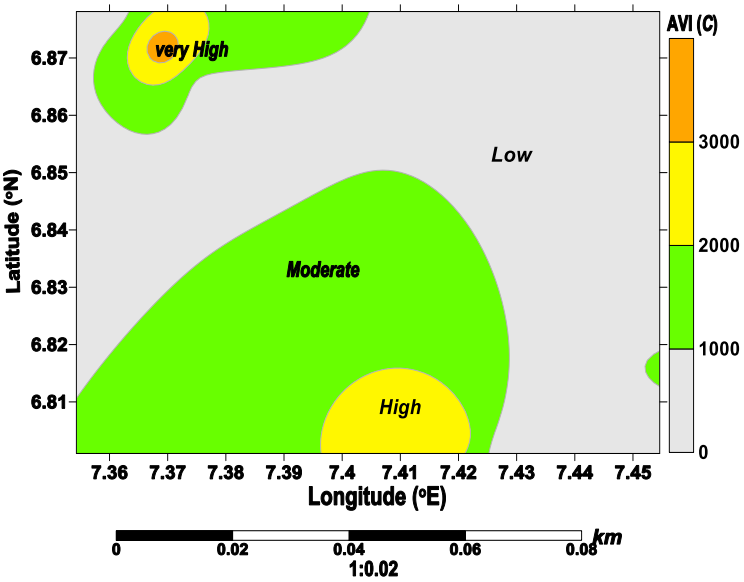

Figure 7: Contour map of AVI

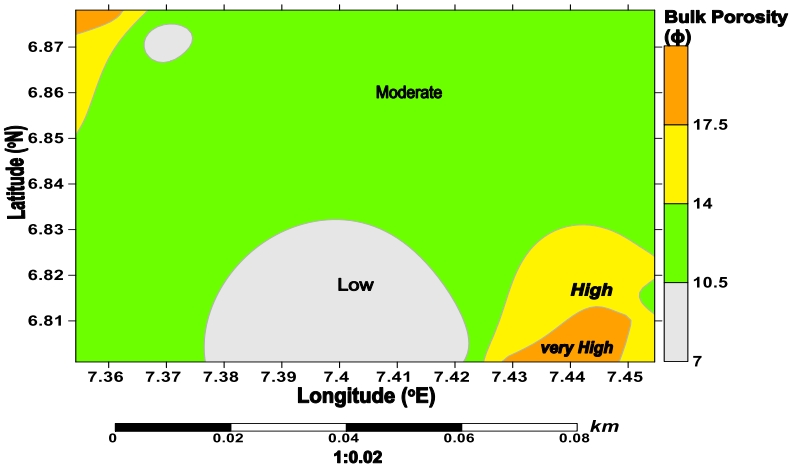

Figure 8: Contour map of porosity

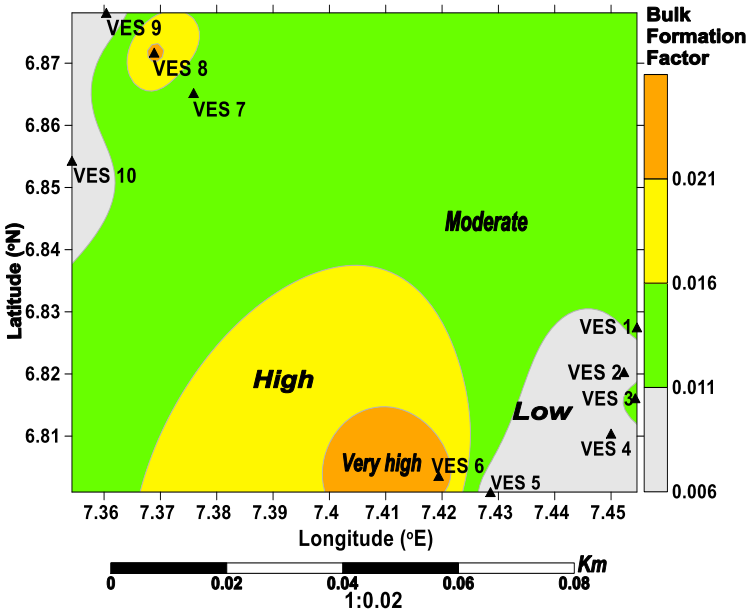

Figure 9: Contour map of Formation facto

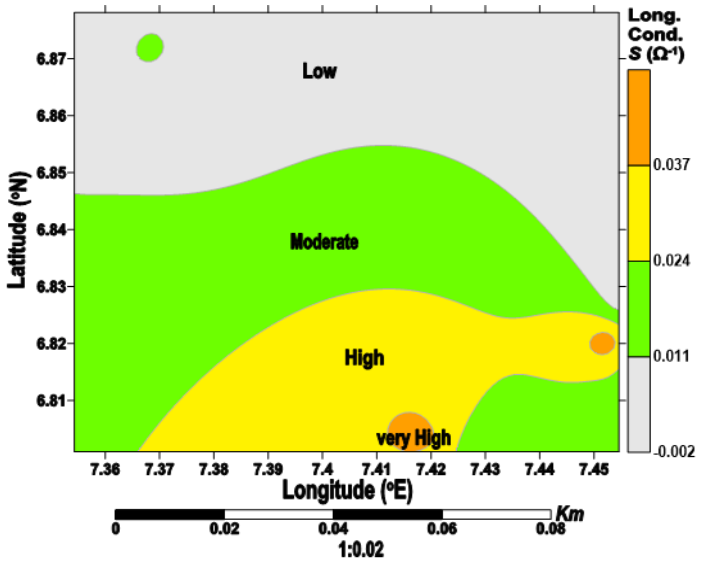

Figure 10: Contour map of longitudinal conductance

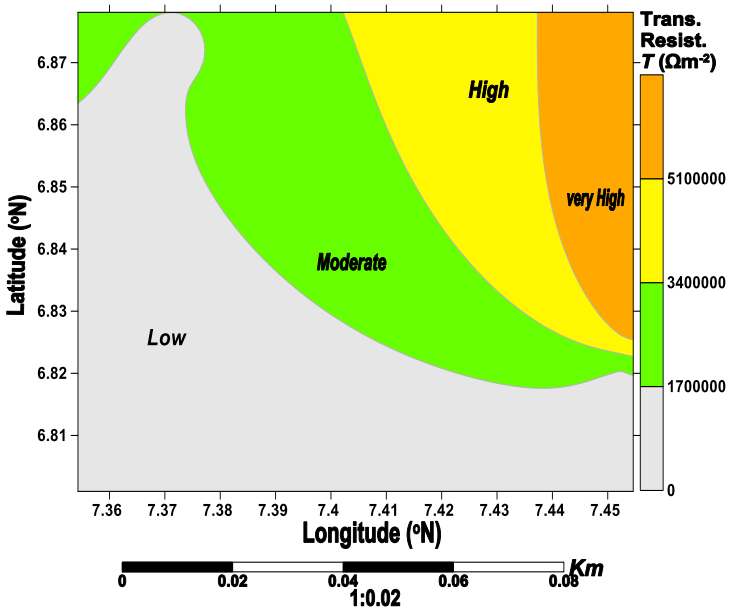

Figure 4.15: Contour map of Transitivity Resistance

The values of longitudinal conductance range from 0.002 to 0.046 Ω^{-1}, with a mean value of 0.024 Ω-1. The results from Table 4 indicate that all the VES points in the study area exhibit poor protective capacities according to the rating in Table 5, suggesting a high susceptibility to contamination of the aquifers in the study area. This finding is consistent with previous studies conducted by group of researchers, highlighting the potential for contamination due to the aquifer materials' high porosity and hydraulic conductivity (Oseji et al., 2020; Ibuot et al., 2019). The contour maps presented in Figure 10 illustrates the spatial distribution of longitudinal conductance in the study area, revealing an increasing trend from north to south. On the other hand, the transverse resistance values range from 41836.86 to 6462359 Ωm^2, with an average value of 1887721 Ωm^2. The contour map depicted in Figure 11 demonstrates that low transverse resistance values are more predominant in the southwest region, gradually increasing towards the northeast.

5. Conclusion

This study investigated the vulnerability of aquifers in parts of Nsukka East and West Local Government Area, Enugu State, Nigeria, using the electrical resistivity method. A total of ten VES points were considered and the analysis revealed five geoelectric layers within the maximum current electrode separation. By analyzing geoelectric parameters like hydraulic conductivity and transverse resistance, along with aquifer vulnerability index, the results gave valuable insights into the groundwater conditions in the area. The results showed that some areas have high potential for extracting groundwater, but they also have low protective capacities, which means they are more at risk of pollution. Also, areas with thicker layers above the aquifer showed higher protective capacities, making them less vulnerable to pollutants.

Table 5: Rating of protective capacity based on GPI (Oladapo et al. 2004)

Geophysically based protection index (GPI) (Ω^{-1})	Protective capacity rating
> 2.0	Strong
1.1 – 2.0	Moderate
0.1 – 1.0	Fair
< 0.1	Weak

References

Amah, J. I., Okoyeh, E. I., Onwuka, S. O., and Amah, J. I., 2016. Statistical modeling of the hydrostratigraphy and hydraulics of the Cretaceous aquifers in Nsukka , North of the Anambra basin , Southeast Nigeria. Advances in Applied Science Research, 7 (4), Pp. 32–41.

Chaudhari, A. N., Mehta, D. J., and Sharma, N. D., 2022. Coupled effect of seawater intrusion on groundwater quality: study of South-West zone of Surat city. Water Supply, 22 (2), Pp. 1716–1734. https://doi.org/10.2166/ws.2021.323

Ezeh, C. C., Ugwu, G. Z., and others., 2010. Geoelectrical sounding for estimating groundwater potential in Nsukka LGA Enugu State, Nigeria. International Journal of Physical Science, 5 (5), Pp. 415–420.

Ezim, E. O., Obiadi, I. I., and Akaegbobi, M. I., 2017. The use of statistical grain-size method in analysing borehole and evaluating aquifer parameters. A case study of Ajali Sandstone formation, southeastern Nigeria. Global Journal of Geological Sciences, 15 (1), Pp. 77. https://doi.org/10.4314/gjgs.v15i1.7

Haritash, A. K., Mathur, K., Singh, P., & Singh, S. K., 2017. Hydrochemical characterization and suitability assessment of groundwater in Baga–Calangute stretch of Goa, India. Environmental Earth Sciences, 76 (9), Pp. 341. https://doi.org/10.1007/s12665-017-6679-5

Ibuot, J. C., Okeke, F. N., Obiora, D. N., and George, N. J., 2019. Assessment of impact of leachate on hydrogeological repositories in Uyo, Southern Nigeria. Journal of Environmental Engineering and Science, 14 (2), Pp. 97–107. https://doi.org/10.1680/jenes.18.00014

International Groundwater Resources Assessment Centre., 2022. What is Groundwater? https://www.un-igrac.org/what-groundwater

Machiwal, D., Jha, M. K., Singh, V. P., and Mohan, C., 2018. Assessment and mapping of groundwater vulnerability to pollution: Current status and challenges. Earth-Science Reviews, 185, 901–927.

Nagkoulis, N., and Katsifarakis, K. L., 2022. Cost minimization of groundwater supply to a central tank. Water Supply, 22 (2), Pp. 2055–2066. https://doi.org/10.2166/ws.2021.298

Ncibi, K., Chaar, H., Hadji, R., Baccari, N., Sebei, A., Khelifi, F., Abbes, M., and Hamed, Y., 2020. A GIS-based statistical model for assessing groundwater susceptibility index in shallow aquifer in Central Tunisia (Sidi Bouzid basin). Arabian Journal of Geosciences, 13 (2), Pp. 98. https://doi.org/10.1007/s12517-020-5112-7

Obiora, D. N., and Ibuot, J. C., 2020. Geophysical assessment of aquifer vulnerability and management: a case study of University of Nigeria, Nsukka, Enugu State. *A*pplied Water Science, 10 (1), Pp. 29. https://doi.org/10.1007/s13201-019-1113-7

Oladapo, M.I., Mohammed M.Z., Adeoye, O.O., and Adetola, O.O, 2004. Geoelectric investigation of the Ondo State Housing Corperation Estate; Ijapo, Akure, southwestern Nigeria; Journal of Mining and Geology, 40 (1), Pp. 41–48.

Onwe, M. R., Abraham, E. M., Ambrose, N. T., and Osike, O. K., 2022. An evaluation of the hydrogeology potential of Nsukka, Southern Nigeria, using geographic information system. Applied Water Science, 12 (4), 1–11. https://doi.org/10.1007/S13201-022-01579-6/TABLES/4

Ossai, M. N, 2020. Vulnerability assessment of hydrogeologic units in parts of Enugu North, Southeastern Nigeria, using integrated electrical resistivity methods. Indian Journal of Science and Technology, 13 (34), Pp. 3495–3509. https://doi.org/10.17485/IJST/v13i34.1366

Singh, L. K., Jha, M. K., and Chowdary, V. M., 2018. Assessing the accuracy of GIS-based Multi-Criteria Decision Analysis approaches for mapping groundwater potential. Ecological Indicators, 91, Pp. 24–37. https://doi.org/10.1016/j.ecolind.2018.03.070

Yee, A. S., and Le, L. N., 2023. Hitting The Ground Flowing: Ways to Sustainably Manage Groundwater Supply and Demand. Asian Development Blog, Straight Talk from Development Experts. https://blogs.adb.org/blog/hitting-ground-flowing-ways-sustainably-manage-groundwater-supply-and-demand